Neurochemistry International 127 (2019) 64–72

Contents lists available at ScienceDirect

Neurochemistry International

journal homepage: www.elsevier.com/locate/neuint

Inhibition of miR-497 improves functional outcome after ischemic stroke by enhancing neuronal autophagy in young and aged rats

Xudong Chen[a], Siyang Lin[a], Lei Gu[a], Xiaohong Zhu[a], Yinuo Zhang[a], Hongxia Zhang[b], Bei Shao[a], Qichuan Zhuge[a], Kunlin Jin[a,b,*]

[a] Zhejiang Provincial Key Laboratory of Aging and Neurological Disorder Research, The First Affiliated Hospital, Wenzhou Medical University, Wenzhou, Zhejiang, 325000, China

[b] Department of Pharmacology and Neuroscience, University of North Texas Health Science Center, Fort Worth, TX, 76107, USA

ARTICLE INFO

Keywords:
Autophagy
Ischemic stroke
MiRNA
Neuroprotection
Aging
miR-497

ABSTRACT

Over the years miR-497 has been found to play a vital role in the pathogenesis of neurological diseases, including ischemic stroke. However, its underlying mechanism remains largely unexplored. Here, we used miR-497 agomir (miR-497 agonist), miR-497 antagomir (miR-497 inhibitor) and 3-MA (autophagy inhibitor) to treat ischemic rats (n = 10–12 per group) induced by permanent distal middle cerebral artery occlusion (dMCAO), followed the functional outcome assessment 24 h after dMCAO. We found that treatment of miR-497 antagomir, but not miR-497 angomir, reduced the infarct volume and improved neurological deficits after ischemic stroke, along with upregulation of the autophagy-related protein LC3 expression (mean ± SEM,$p < 0.05$). While the ischemic rats treated with 3-MA exhibited inhibition of autophagy, which in turn abolished functional recovery as observed in miR-497 antagomir-treated group ($p < 0.05$). Interestingly, the role of miR-497 in functional recovery in aged ischemic rats was less effective, compared to young adult ischemic rats ($p < 0.05$). Our data suggest that inhibition of miR-497 could protect cerebral ischemic injury by enhancing autophagy and also age-dependent.

1. Introduction

Stroke remains a leading cause of disability worldwide and the 5th leading cause of death in the Unites States. About 15 million people suffer stroke worldwide each year (Roitbak, 2018; Ruan et al., 2015), and ischemic stroke accounts for about 70% of all stroke cases. Although stroke occurs at any age, but nearly three-quarters of all strokes occur in people over the age of 65. Recombinant tissue plasminogen activator (rtPA) have been approved to use for thrombolytic therapy within 4.5 h after onset of ischemic stroke (Wang et al., 2018; Zhang and Chopp, 2009). Due to limited time window, only a few patients with ischemic stroke can benefit from the rtPA treatment. Although advances are proceeding on several fronts, which include intra-arterial fibrinolysis (Ogawa et al., 2007) and mechanical clot removal systems such as the Merci clot retrieval device and the Penumbra system (Segura et al., 2008), these devices can only remove clot from proximal sites such as the distal internal carotid artery or proximal middle cerebral artery, but not more distal clots and therefore are unable to be applied to the majority of stroke patients. There is therefore an urgent need for more effective, safe and feasible therapeutic method for ischemic stroke, especially in the acute stage (Descloux et al., 2015; Love, 2003; Yuan, 2009). As ischemic stroke mainly occurs in the aged population (Arnold, 1981; Ramirez-Lassepas, 1998; Xu et al., 2017), it is important to know how aging impact the outcome after treatment.

MicroRNAs (miRNAs) are small non-coding RNAs approximately 22 nucleotides in length that are highly conserved through evolution. They play a critical role in post-transcriptional gene regulation by binding to complementary sites in the 3′-untranslated region (3′-UTRs) of mRNAs (Bartel, 2009), which involves in the regulation of a variety of cellular processes such as neuronal development, differentiation, synaptic plasticity, proliferation, metabolism, and apoptosis (Johnnidis et al., 2008). Growing evidence supports that miRNA also plays roles in several human diseases, from cancer to cardiovascular disease. In recent years, many studies have reported that miRNAs have key roles in the pathophysiological processes contributing to ischemic stroke injuries (Tao et al., 2015; Wu et al., 2012). For example, upregulation of miR-107 in the ischemic brain could inhibit glutamate transporter-1 (GLT-1) expression and elevated glutamate accumulation (Yang et al., 2014),

* Corresponding author. Zhejiang Provincial Key Laboratory of Aging and Neurological Disorder Research, The First Affiliated Hospital, Wenzhou Medical University, Wenzhou, Zhejiang, 325000, China.
E-mail address: kunlin.jin@unthsc.edu (K. Jin).

https://doi.org/10.1016/j.neuint.2019.01.005
Received 30 November 2018; Received in revised form 4 January 2019; Accepted 7 January 2019
Available online 15 January 2019
0197-0186/

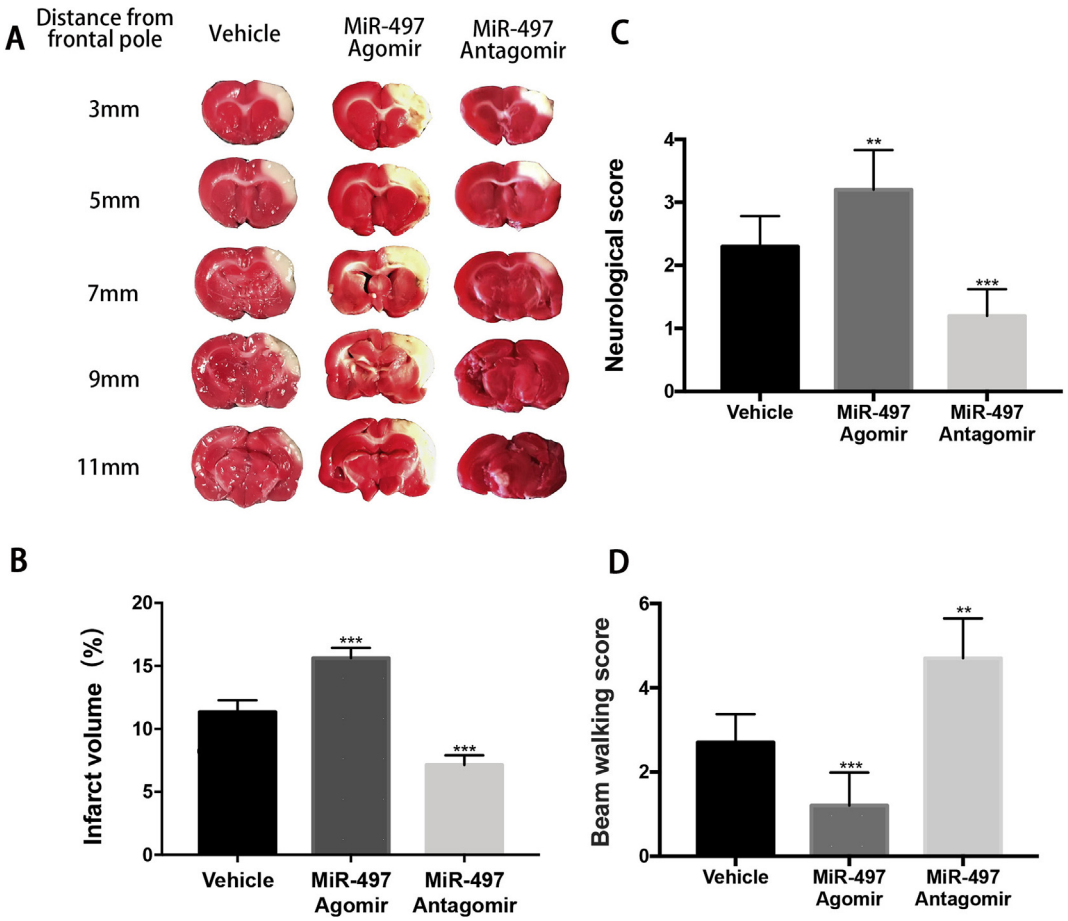

Fig. 1. MiR-497 treatment exacerbated infarct volume and neurological deficits after dMCAO. A) Representative images of infarct areas determined by TTC staining 24 h after dMCAO in the rats treated with miR-497 agomir, antagomir or vehicle. **B)** Statistic data of infarct volume after dMCAO followed treatment of miR-497 agomir, antagomir or vehicle. N = 6 per group. **C)** Neurologic deficit score 24 h after focal ischemia. N = 10–12. **D)** Beam balance test scores 24 h after focal ischemia followed miR-497 agomir or antagomir treatment. N = 10–12 per group. The data were expressed as mean ± SD. $^{**}P < 0.01$; $^{***}P < 0.001$ vs vehicle group.

which are critical in the excitotoxicity of neuronal cells, after focal ischemia. Similarly, miR-223 overexpression inhibited N-methyl-D-aspartic acid receptor (NMDA)-induced calcium influx in hippocampal neurons and protected the ischemic brain from excitotoxic injury through suppression the levels of the glutamate receptor-2 (GluR2) and NMDA subunit NR2B (Harraz et al., 2012). MiR-497 is another critical player in the regulation of neuronal death after focal ischemia. MiR-497 was found to be induced in mouse brain transient focal ischemia, and MiR-497 overexpression promotes neuronal death after ischemia by inhibits bcl-2 and bcl-w expression. Inhibition of miRNA-497 using antagomirs was found to lower miR-497 levels and therefore ameliorates infarct volume and improve neurological deficits in brain (Yin et al., 2010). However, its underlying mechanism is still not well understood.

In this study, we investigated the underlying mechanism of miR-497 in functional outcome after focal ischemia. We found that miR-497 exacerbated infarct volume and neurological deficits through inhibiting Bcl-2 and microtubule-associated protein 1A/1B-light chain 3 (LC3), the latter is critical in autophagy process. Inhibiting autophagy could abolished the effect of miR-497 on the functional outcome after focal ischemia. In addition, we also documented that the impact of miR-497 on the ischemic outcome was age-dependent. Our data uncover new pharmacological mechanism of miR-497 in functional outcome after ischemic stroke.

2. Materials and methods

2.1. Ischemic stroke model and miRNA injection

Male adult (2-months-old, and 5-6-months-old) Sprague-Dawley rats were purchased from the Animal Center of Shanghai Branch, Chinese Academy of Sciences and maintained at the Experimental Animal Center of Wenzhou Medical University. Some of them housed in a standard animal room until 12–15-months old. We used 12-15-months-old rats, as ischemic stroke mainly occurs in the elderly (> 65 years) and 12-months-old rats equals to 52 human years (http://www.age-converter.com/rat-age-calculator.html). All animal experiments were approved by the Laboratory Animal Ethics committee of Wenzhou Medical University and performed in accordance with the *National Institutes of Health Guide for the Care and Use of Laboratory Animals.* Animals were housed in a temperature- and humidity-controlled animal facility with a 12-h light–dark cycle. Food and water were available *ad libitum*. All efforts were made to minimize animal suffering and the number of animals killed.

Focal cerebral ischemic stroke model was procedure by permanent distal middle cerebral artery occlusion (dMCAO) method, plus ipsilateral common carotid artery (CCA) occlusion as described before. Briefly, rats were anesthetized with 10% chloral hydrate (3.5 ml/kg, intraperitoneal injection). A vertical skin incision at the midline of the neck was made to separate the two lateral common carotid arteries (CCA). A 2-cm incision was then cut between the right orbit and tragus

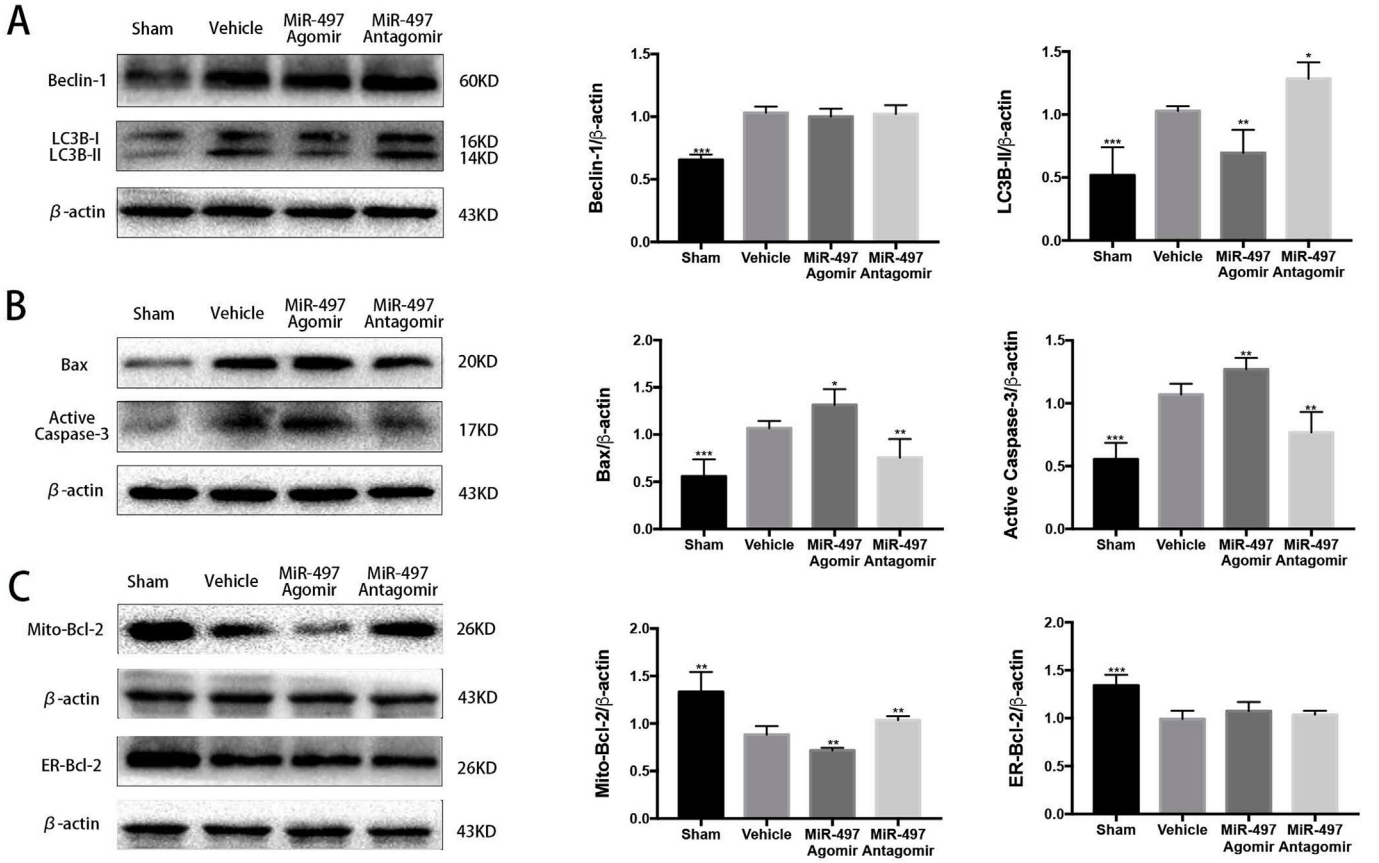

Fig. 2. The effect of MiR-497 treatment on the expression levels of autophagy- and apoptosis-related proteins in the ischemic brain. A) Western blot (left panel) shows the expression levels of autophagy-related beclin-1 and LC3B-II protein after miR-497 antagomir or angomir treatment. Quantification of Beclin-1 and LC3B-II proteins (middle and left panel). **B)** The expression levels of Bax and Caspase-3 proteins after treatment of miR-497 antagomir or angomir (left panel). Quantification of Bax and active Caspase-3 proteins after injection of miR-497 antagomir or angomir (middle and left panel). **C)** The effect of miR-497 antagomir or angomir on expression level of Bcl-2 protein located in mitochondria and endoplasmic reticulum (ER) (right panel). Quantitation of Mito-Bcl-2 and ER-Bcl-2 was shown in middle and left panels. The data were expressed as mean ± SD. N = 4–5/group. *P < 0.05; **P < 0.01; ***P < 0.001 vs vehicle group.

allowing for removal of temporalis muscle to exposed skull, followed by a 3-mm diameter round hole drilled on the skull with a microdrill to reveal the visible middle cerebral artery (MCA). The dura and arachnoid were carefully peeled with tweezers under the surgical microscope, ligated the two lateral CCA and then the right middle cerebral artery was occluded with electrocoagulation without damaging the brain surface. After 60 min, the two lateral CCA were released and the incision sutured. Sham-operated rats underwent identical surgery except that the distal MCA was not occluded. Rectal temperature was maintained at 37.0 °C ± 0.5 °C during surgery with a temperature-regulated heating pad.

MiR-497 (antagomir and agomir) was purchased from GuangZhou Ribobio, and 3-MA (autophagy inhibitor) was obtained from Selleck Chemicals. Sham-operated and ischemic rats were treated with 5 pmol/g miR-497 agomir, antagomir, or 2 nmol/g 3-MA dissolved in 10 μl saline (Jing et al., 2012; Xu et al., 2015), which were intracranially injected into the ischemic core (−0.3 mm posterior to the bregma, 3 mm lateral to midline, 1.8 mm below the dura) for 3–5 min 1 h after focal ischemia using a Hamilton syringe by stereotaxic coordinates (Jin et al., 2010; Le et al., 2011). The needle was slowly withdrawn after injection and, bone defect filled up with bone wax. Then animals were replaced to their cages for recovery from anesthesia.

2.2. Infarct volume measurements

24 h after dMCAO, the brains were removed and sliced into 5 pieces by a brain matrix. Sections were then immersed in prewarmed 2% 2,3,5-Triphenyltetrazolium chloride (TTC, Sigma) in saline for 30 min, and then fixed in 4% paraformaldehyde overnight. The infarct volume was determined on these TTC sections using Image pro plus 5.1 software. The actual infarct volume with edema correction was calculated as the volume of the contralateral hemisphere minus the non-infarcted volume of the ipsilateral hemisphere.

2.3. Neurobehavioral tests

Rats (N = 10–12 per group) underwent neurobehavioral tests to evaluate functional outcome. Animals were trained prior to dMCAO and deficits were assessed 24 h thereafter. The investigator performing the tests was blinded to the experimental condition.

2.3.1. Neurological severity score (NSS)

NSS was performed according to previous published papers (Longa et al., 1989). NSS was a five-point scale. 0, rat was normal; 1, rat failed to extend left forepaw; 2, rat circled to left; 3, rat fell to the left; 4, no spontaneous movement.

2.3.2. Beam walking test

The beam-walking test was used to assess deficits in coordination and integration of motor movement, especially in the hindlimb, and performed as previously described with modification. Rats were placed on a square wooden beam (2.0 × 2.0 × 120 cm) at a height of 50 cm from ground. The scoring criteria was as follows: 0 score, rat fell from wood; 1 score, rat was unable to move only can keep on the wood; 2

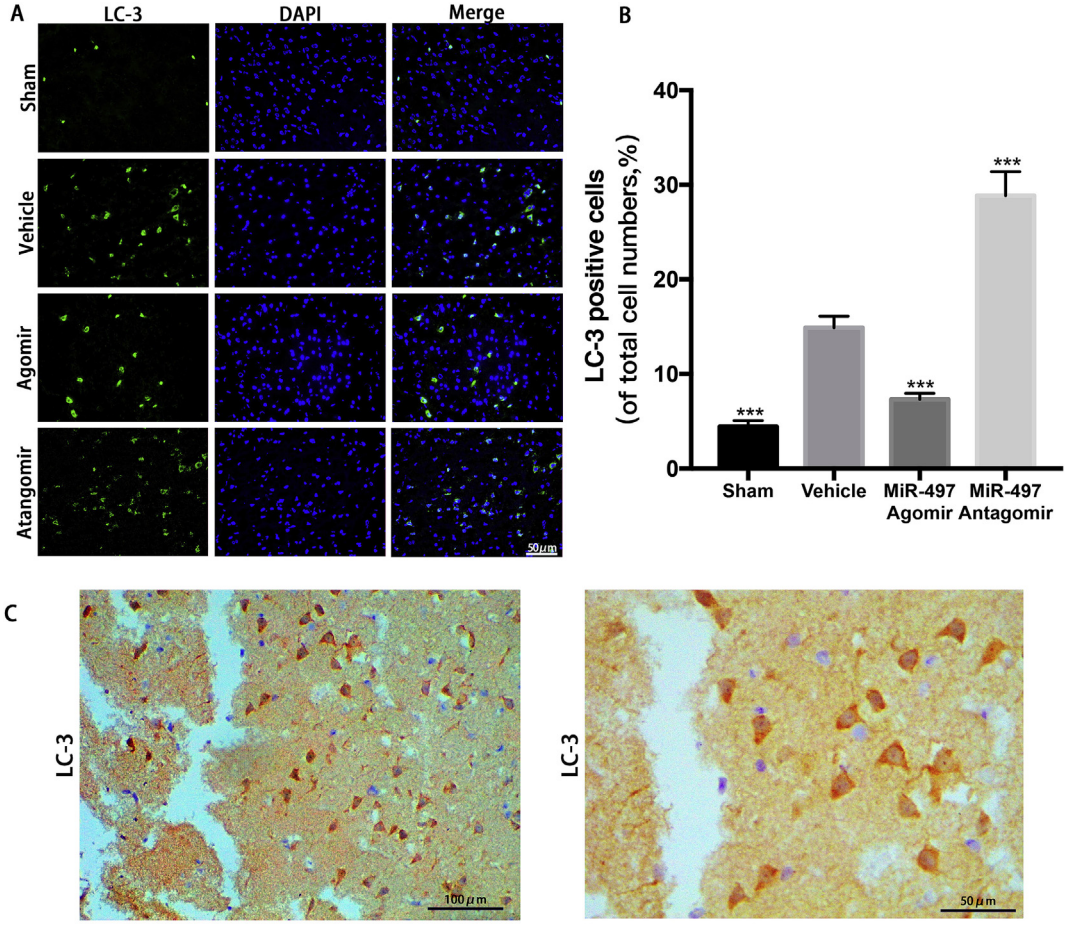

Fig. 3. The effect of MiR-497 treatment on the immunohistochemical pattern of LC3 after ischemia stroke. A) Immunohistochemical evidence for autophagy-related protein LC3 (green) expression in the peri-infarct regions after miR-497 antagomir or angomir treatment. Nuclei were counterstained with DAPI (blue). **B)** Quantitation of LC3 in the peri-infarct regions in the group treated with miR-497 agomir and atangomir. **C)** Representative images of LC3 immunoreactivity in the peri-infarct regions. Left: low-magnification view; right: high-magnification view. The data were expressed as mean ± SD. N = 4–5/group. ***P < 0.001, vs vehicle group.

scores, rat turned to left or right side but unable to move forward on the wood; 3 scores, rat could pass the wood with more than half hindlimb-slips of total steps; 4 scores, rat passed it with less than half hindlimb-slips of total; 5 scores; rat passed the wood without any slips of the hindlimb. Rats were placed on the beam for three consecutive times and the mean of three used.

2.4. Western blot

The cerebral cortex was dissected and lysed in RIPA lysis buffer containing PMSF (100:1, Beyotime). To investigate subcellular distribution of proteins, mitochondria and endoplasmic reticulum fractions were enriched using tissue Mitochondrial Extraction Kit (Beyotime) and Endoplasmic reticulum Isolation Kit (Sigma), respectively. Protein were separated by 12% SDS polyacrylamide gels and transferred with nitrocellulose membranes. The membranes with proteins were blocked with 5% milk in TBST (0.1% Tween20 in 1 × Tris buffered saline) at room temperature for 1–3 h. Then membranes were incubated with one of primary antibodies against rabbits Beclin-1 (1:1000; CST), LC3B (1:1000; CST), Bcl-2 (1:1000, Abcam), Bax (1:1000, Abcam), active Caspase-3 (1:500, Abcam) or β-actin (1:1000, Abcam) at 4 °C overnight. Membrane was washed with TBST three times for every 15 min and incubated at room temperature for 60 min with horseradish peroxidase conjugated with horseradish peroxidase conjugated goat anti-rabbit (1: 3,000, Santa Cruz Biotechnology), and thereafter washed three times for 15 min with PBS/Tween 20. Peroxidase activity was visualized by chemiluminescent HRP substrate (Thermo Scientific). The signal was quantified with Image Lab software 5.2.1 (Bio-Rad Laboratories) and normalized using β-actin (1:1000, Abcam) loading control.

2.5. Immunohistochemistry

Immunohistochemistry was performed as described previously (Hwang et al., 2016; Li et al., 2016). Rats were perfused with 60–100 ml normal saline followed by 100–150 ml 4% paraformaldehyde. Brains were fixed with in paraformaldehyde for 2 days, and then embedded in paraffin. Some brains were also fixed in 4% paraformaldehyde for 1 day and then dehydrated in 30% sucrose solutions for 2 day. Brains were embedded in O.C.T. Compound and cut into 6–8 μm frozen section. Immunohistochemistry was performed as described previously (Refs). In brief, endogenous peroxidase activity was blocked by incubation in 3% H_2O_2 for 30 min at room temperature. After several washes with PBS, the sections were incubated in blocking solution (5% Goat Serum Albumin; Sigma) for 1 h. Brains were incubated with primary antibodies, including anti-LC3B (1:200, CST), rabbit anti-caspase-3 (1:200, Abcam), or mouse anti-NeuN (1:150, Novus) at 4 °C overnight. After washing, the sections were incubated with a mixture solution containing goat anti-rabbit FITC and goat anti-mouse DyLight 594 (1:400, Earth) for 1 h at room temperature. The sections were washed 3 times by PBS after incubation and stained with DAPI (Solarbio) for 10 min. Finally, the immunopositive cells were observed with a fluorescent

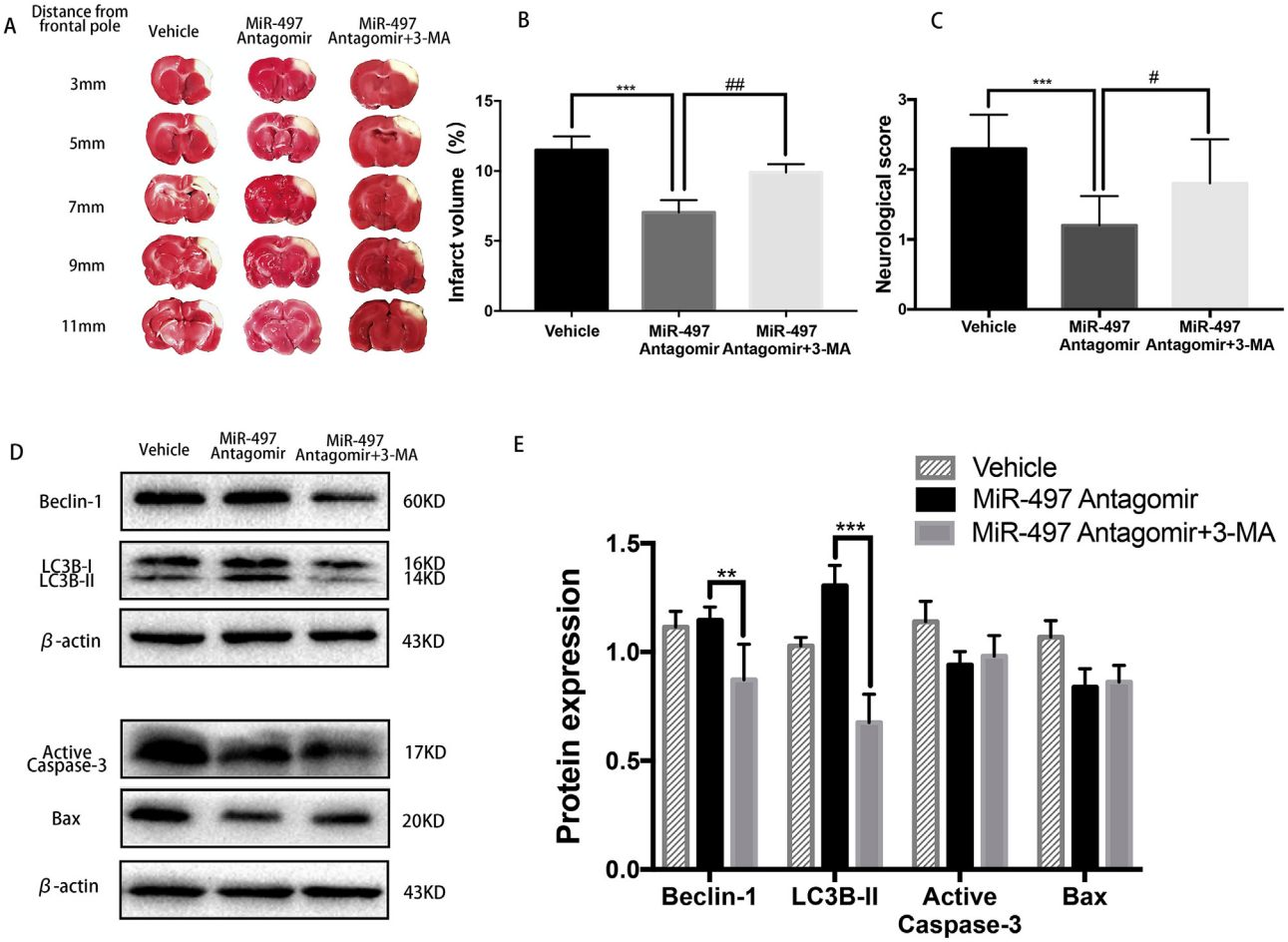

Fig. 4. The inhibition of MiR-497 ameliorated the ischemic outcome by enhancing autophagy. A) Representative images of TTC-stained brain sections show the infarct areas after treatment of miR-497 antagomir, 3-MA and vehicle. **B)** Statistic data of infarct volume after dMCAO followed treatment of miR-497 antagomir, 3-MA or vehicle. N = 6 per group. **C)** Neurologic deficit score was improved in the group treated miR-497 antagomir and 3-MA, compared to the group treated with miR-497 antagomir only. N = 10 per group. **D)** Western blots show the expression levels of beclin-1, LC3B-II, Bax and active Caspase-3 after treatment of miR-497 antagomir, 3-MA or vehicle. **E)** Quantitation analysis of proteins in panel D. The data were expressed as mean ± SD. ***P < 0.001, vs vehicle group; #P < 0.05, ##P < 0.01, vs miR-497 antagomir group.

microscopy (Leica). Controls included omitting the primary or secondary antibody.

2.6. Statistical analysis

Quantitative results were expressed as mean ± SD. The statistical significance of difference between means was evaluated using Student's *t*-test or analysis of variance (ANOVA), followed by Newman–Keuls *post hoc* tests. Behavioral data were analyzed by two-way analysis of variance (ANOVA) with repeated measures, followed by *post hoc* multiple comparison tests (Fisher PLSD or Student's paired *t*-test with the Bonferroni correction). *P* values < 0.05 was considered significant.

3. Results

To determine if miR-497 played a role in functional outcome after focal ischemia, initially, miR-497 antagomir or agomir at high concentration was intraperitoneally injected 1 h after focal ischemia and outcome was determined 24 h after treatment. Interestingly, no significant outcome improvement was found in the group treated with miR-497 antagomir, compared with the groups treated with miR-497 agomir or vehicle. We expected that the concentration of miR-497 in the ischemic regions was too low to execute the function if miR-497 was intraperitoneally injected. Then, we tested the intracranial injection of miR-497 antagomir, agomir or vehicle into the ischemic core 1 h after focal ischemia. 24 hr after dMCAO, we found that knockdown of miR-497 effectively exacerbated the infarct volume and neurological deficits, compared with the vehicle group (Fig. 1 However, after miR-497 antagomir treatment, the infarct volume was significantly reduced, and motor function impairment was improved (Fig. 1). Our data suggest that MiR-497 inhibition exacerbated outcome after acute ischemic stroke.

Next, we explored the mechanism underlying miR-497-mediated neuroprotection after focal ischemia. By Western blot analysis, we confirmed that apoptotic genes Bax and activated form of caspase-3 were significantly increased in the ischemic brain 24 h after miR-497 agomir injection (Fig. 2B) (Yin et al., 2010). Interestingly, miR-497 agomir treatment only inhibited mitochondrion-targeted bcl-2 expression, but not ER-targeted Bcl-2 (Fig. 2C). We then asked whether autophagy was the upstream signaling of these apoptotic genes. Beclin-1 is at the midstream and LC3 is at the downstream in autophagy pathway (Ginet et al., 2014). We found that LC3 expression was reduced in the group treated with miR-497 agomir but increased in the group treated with miR-497 antagomir, compared with vehicle group (Fig. 2A). To determine the patterns of LC3 protein, immunocytochemistry was performed. Fig. 3 illustrates that LC3-immunopositive cells were increased in the peri-infarct regions after focal ischemia, compared with sham-operated control. The number of LC3-immunopositive cells were

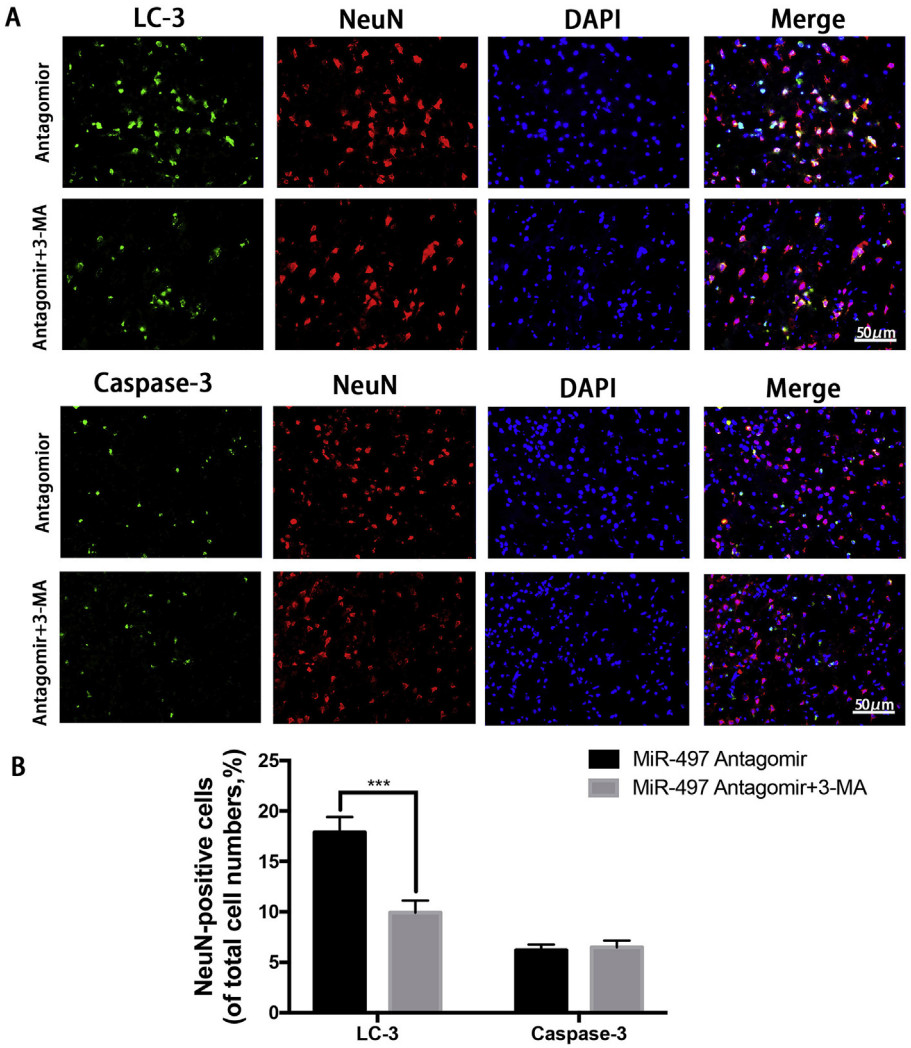

Fig. 5. The MiR-497 antagomir predominantly affects on neuronal autophagy but not neuronal apoptosis after focal ischemia. A) Representative images of LC3 (top panels) and Caspase-3 (bottom panels)-immunpositive cells expressed NeuN (red) protein in the peri-infarct regions after treatment of miR-497 antagomir, 3-MA and vehicle. Nuclei were counterstained with DAPI (blue). **B)** Quantitation analysis of LC3/NenN or Caspase-3/NeuN cells after treatment. The data were expressed as mean ± SD. N = 4–5 per group. ***P < 0.001, vs vehicle group.

significantly increased after miR-497 antagomir treatment but reduced after miR-497 antagomir (Fig. 3), consisting with the Western blot finding.

Then, we asked whether miR-497 directly targeted autophagy after ischemic stroke. The ischemic rats were treated with miR-497 antagomir with or without autophagy inhibitor, 3-MA. The infarct volume and neurological scores were assessed 24 h after treatment. We found that the reduced infarct volume after inhibition of miR-497 was abolished in the group treated with 3-MA (Fig. 4A and B). Similarly, the improved neurological deficit was also eliminated after 3-MA treatment (Fig. 4C). The findings suggest that inhibiting autophagy attenuates functional recovery at the early stage of ischemic stroke after miR-497 antagomir. Consistently, our Western blot data confirmed that 3-MA inhibited the expression of autophagy markers LC3B and Beclin-1. While apoptotic protein markers Bax and activated form of caspase-3 were not significantly changed after 3-MA treatment (Fig. 4D and E). To determine the phenotype of the LC3-immunopositive cells in the ischemic brain, double immunostaining was performed. As shown in Fig. 5A and B, most LC3-immunopositive cells after miR-497 antagomir treatment expressed NeuN protein, suggesting that autophagy mainly occurred in the neuronal cells. Similarly, knockdown of miR-497 did not significantly affect the number of neuronal apoptotic cells in the peri-infarct regions after focal ischemia (Fig. 5).

As ischemic stroke primarily occurs in the elderly, we asked whether differential effect of miR-497 on ischemic outcome was age-dependent. Same dose of miR-497 antagomir was intracranially injected into the ischemic regions in young and aged rats and the outcome was determined 24 h after ischemia. First, we confirmed that larger infarct volume was found in the aged ischemic rats, in parallel with worsen neurological deficit, compared to young ischemic rats (Fig. 6). Although miR-497 antagomir treatment reduced the infarct volume and increased neurological scores in both young and aged rats after focal ischemia, less effect was found in the aged ischemic rats (Fig. 6). The findings suggest that miR-497 inhibition-mediated neuroprotection is age-dependent.

4. Discussion

The major findings of the present study are (1) that inhibition of miR-497 reduced the infarct volume and improved neurological deficits after ischemic stroke, along with increased autophagy-related protein LC3 expression; (2) while miR-497 agomir treatment reduced LC3 expression and deteriorated infarct volume and neurological deficits; (3) inhibiting autophagy could abolish functional recovery after miR-497 antagomir treatment; and (4) the functional recovery in aged ischemic rats after miR-497 antagomir treatment was less effective, compared to

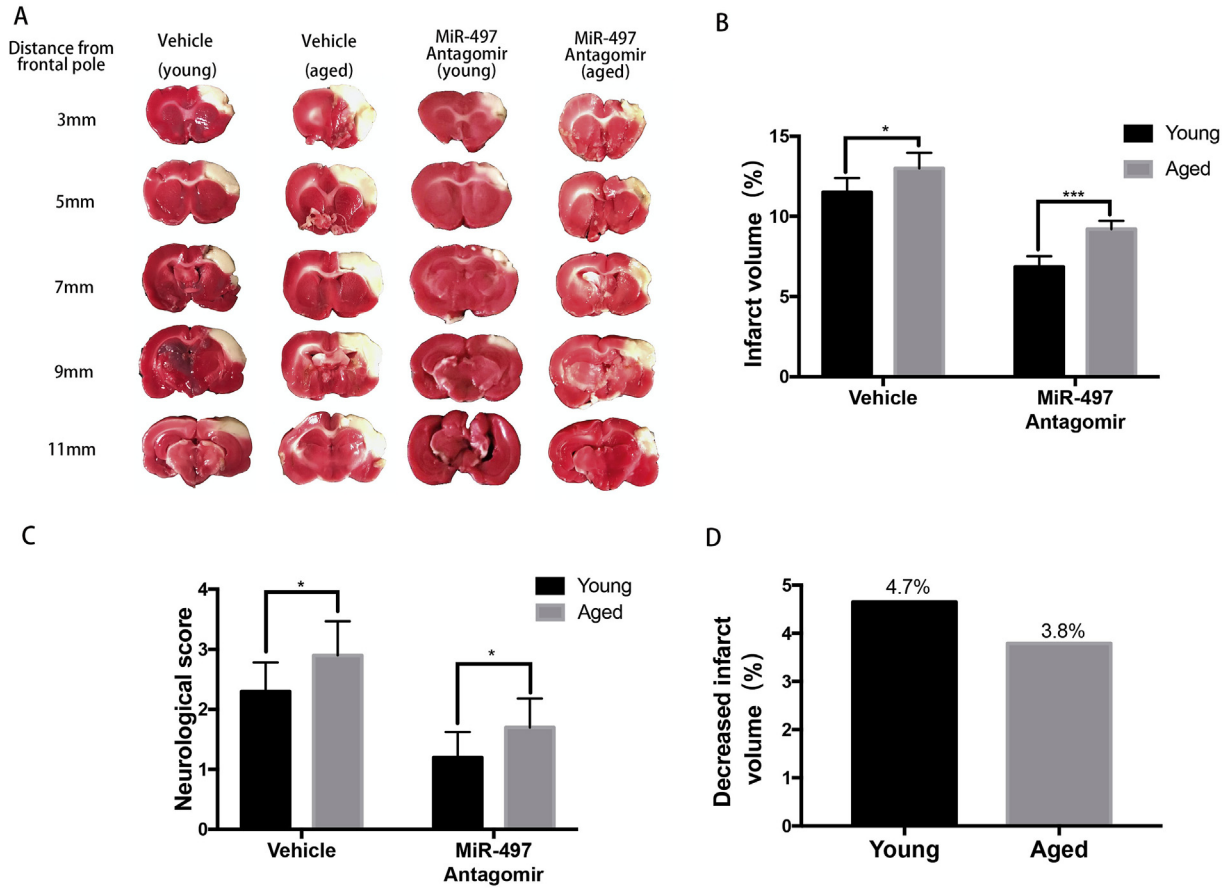

Fig. 6. The effect of MiR-497 on ischemic outcome is age-dependent. A) Representative images of TTC-stained infarct areas in 2- and 12-15-months-old rats after treatment of miR-497 antagomir. **B)** Quantitation analysis of infarct volume in 2- and 12-15-months-old rats after dMCAO followed treatment of miR-497 antagomir. N = 6. **C)** Neurologic deficit scores 24 h after focal ischemia followed treatment of miR-497 antagomir. N = 10 rats/group. **D)** Quantitation analysis of decreased infarct volume after treatment of miR-497 antagomir in 2- and 12-15-months-old ischemic rats. The data were expressed as mean ± SD. **P < 0.01, ***P < 0.001, vs vehicle group.

young adult ischemic rats. Our data suggest that inhibition of miR-497 may protect cerebral ischemic injury through enhancing autophagy, which is also age-dependent.

Previous studies have reported that knockdown of cerebral miR-497 attenuates ischemic brain infarction and improves neurological outcomes in mice after focal cerebral ischemia by enhancing Bcl-2 and Bcl-w protein levels in the ischemic region (Yin et al., 2010). In agreement with these findings, our data demonstrated that inhibition of miR-497 improved the functional outcome after focal ischemia in rats, along with upregulation of Bcl-2 and mitochondrion-restricted Bcl-2 and downregulation of activated form of caspase-3. However, ER-restricted Bcl-2 and the other apoptotic genes such as Bax, were not significantly affected after treatment of either miR-497 antagomir (miR-497 inhibitor) or miR-497 agomir (miR-497 agonist). Bcl-2 family members comprise a group of proteins that regulate apoptosis (Chan et al., 2018; Fernández et al., 2018; Sinoy et al., 2017). The Bax subfamily has been implicated as the “gateway” to apoptosis (Wei et al., 2001). Studies have shown that Bax is regulated by ER-restricted Bcl-2 (Thomenius and Distelhorst, 2003). Our data indicate that mitochondrion-restricted Bcl-2, but not ER-restricted Bcl-2, is required to initiate miR-479-induced neuronal apoptosis after focal ischemia.

Another exciting finding of this study is that the role of miR-497 inhibition in functional outcome after ischemia accompanied by an enhancement of autophagy based on the Western blot and immunostaining data after injection of miR-497 antagomir or agomir. After administration of 3-MA, an inhibitor of autophagy, the enhancement of autophagy can be inhibited, which in turn abolished functional recovery after miR-497 antagomir treatment. In line with our results, Wen et al. (2008) reported that autophagy was activated after focal ischemia, and the infarct volume and motor deficits could be significantly reduced after 3-MA treatment (Wen et al., 2008). The 3-MA-mediated neuroprotective effects were associated with an inhibition of LC3-II. Xin et al. (2011) confirmed that 3-MA treatment could prevent pyramidal neuron death after ischemia (Xin et al., 2011). Thus, our findings are in consistent with previous reports that treatment with 3-MA inhibited autophagy and reversed neuroprotection after stroke (Park et al., 2009; Su et al., 2014). Autophagy is an important normal physiological process in the body to maintains homeostasis or normal functioning by protein degradation and turnover of the destroyed cell organelles for new cell formation (Yamamoto and Yue, 2014). In addition to necrosis and apoptosis, autophagy has also been implicated in the pathogenesis of ischemic stroke (Descloux et al., 2015; Klionsky, 2010), although autophagy has been considered as a double-edged sword for neuronal survival after cerebral ischemia (Carloni et al., 2008; Wang et al., 2018; Yamamoto and Yue, 2014). Carloni et al. (2010) suggested that autophagy may be an integrated pro-survival signaling. When autophagy was interrupted, cells underwent necrotic cell death. Consistenntly, Chen et al. (2014) reported that autophagy induced by nicotinamide phosphoribosyltransferase (Nampt) promoted neuronal survival after cerebral ischemia. Other studies have suggested moderate autophagy may improve the outcome of stroke (Wang et al., 2014), but others also pointed long term autophagy would cause excessive cell death exacerbating ischemic stroke injury (Baek et al., 2014; Lv et al., 2017; Wang et al., 2017; Xu et al., 2017). Therefore,

whether autophagy is beneficial or deleterious depended on the degree and duration of autophagy (Wang et al., 2018). Our data suggest that autophagy could be beneficial for stroke in the early stage.

We believe, neuronal autophagy probably is a major part of survival mechanism of acute cerebral ischemia (Carloni et al., 2010). Studies have reported that Bcl-2 not only functions as an anti-apoptotic protein, but also as an anti-autophagy protein via its inhibitory interaction with Beclin-1 (Llambi et al., 2016; Pattingre et al., 2005). A very recent study shows that the expression of miR-30d-5p could significantly inhibit both Beclin-1 and Atg5 expression, and inhibition of autophagy transformed microglial/macrophage polarization from M1 to M2 after ischemia (Jiang et al., 2018). Interestingly, our data showed that inhibition of miR-497 did not affect the expression levels of Beclin-1 rather than LC3. In addition, MiR-497 affected on mitochondrion-targeted Bcl-2 but not ER-targeted Bcl-2. The findings suggest that the target of miR-497 in autophagy pathway may directly act on LC3, which are mostly concentrated in neurons, not through the Bcl-2/Beclin-1 signaling.

As ischemic stroke mainly occurs in the elderly, it is important to know whether similar effect in young ischemic models is also observed in aged ischemic model, which is critical for clinical translation (Pan et al., 2017). There is a universal understanding that many of treatment options are more effective in young population but lessen the aged ones (Aurel et al., 2007; Yang and Paschen, 2017). Yet, no mathematical formula to precisely calculate the human age of a rat because its growth and physiological changes during its life are very different from humans. Based on the online database (www.age-converter.com/rat-age-calculator.html), 12-months-old equals to 52 human years. Reports indicate that 75–89% of strokes occur in individuals aged > 65 years (Strong et al., 2007). In order to verify the similar impact of miR-497 on functional outcome in 12-15-months-old ischemic rats, miR-497 antagomir or vehicle was injected into young or aged ischemic rats and outcome was assessed 24 h after ischemic stroke. We found that although inhibition of miR-497 could improve the infarct volume and neurological deficits in aged ischemic rats, but less effective compared to young (2-months-old) ischemic rats. The findings suggest that age is important factor for experimental design, which may maximize the success rate from bench to bedside.

Acknowledgements

This work is supported by Key Laboratory of Aging and Neurological Disorder Research of Wenzhou Medical University, China.

Appendix A. Supplementary data

Supplementary data to this article can be found online at https://doi.org/10.1016/j.neuint.2019.01.005.

References

Arnold, K.G., 1981. Cerebral blood flow in geriatrics–a review. Age Ageing 10, 5–9.
Aurel, P.-W., Stanley Thomas, C., Zaal, K., Christof, K., Lary, C.W., 2007. The response of the aged brain to stroke: too much, too soon? Curr. Neurovascular Res. 4, 216–227.
Baek, S.H., Noh, A.R., Kim, K.A., Akram, M., Shin, Y.J., Kim, E.S., Yu, S.W., Majid, A., Bae, O.N., 2014. Modulation of mitochondrial function and autophagy mediates carnosine neuroprotection against ischemic brain damage. Stroke 45, 2438–2443.
Bartel, D.P., 2009. MicroRNAs: target recognition and regulatory functions. Cell 136, 215–233.
Carloni, S., Buonocore, G., Balduini, W., 2008. Protective role of autophagy in neonatal hypoxia-ischemia induced brain injury. Neurobiol. Dis. 32, 329–339.
Carloni, S., Girelli, S., Scopa, C., 2010 Apr. Activation of autophagy and Akt:CREB signaling play an equivalent role in the neuroprotective effect of rapamycin in neonatal hypoxia-ischemia. Autophagy 6 (3), 366–377.
Chan, S.J., Zhao, H., Hayakawa, K., Chai, C., Tan, C.T., Huang, J., Tao, R., Hamanaka, G., Arumugam, T.V., Lo, E.H., Yu, V.C.K., Wong, P.H., 2018. Modulator of apoptosis-1 is a potential therapeutic target in acute ischemic injury. J. Cerebr. Blood Flow Metabol., 271678X18794839.
Chen, W., Sun, Y., Liu, K., Sun, X., 2014. Autophagy: a double-edged sword for neuronal survival after cerebral ischemia. Neural. Regen. Res. 9 (12), 1210–1216.
Descloux, C., Ginet, V., Clarke, P.G.H., Puyal, J., Truttmann, A.C., 2015. Neuronal death after perinatal cerebral hypoxia-ischemia: focus on autophagy—mediated cell death. Int. J. Dev. Neurosci. 45, 75–85.
Fernández, Á.F., Sebti, S., Wei, Y., Zou, Z., Shi, M., McMillan, K.L., He, C., Ting, T., Liu, Y., Chiang, W.-C., Marciano, D.K., Schiattarella, G.G., Bhagat, G., Moe, O.W., Hu, M.C., Levine, B., 2018. Disruption of the beclin 1–BCL2 autophagy regulatory complex promotes longevity in mice. Nature 558, 136–140.
Ginet, V., Spiehlmann, A., Rummel, C., Rudinskiy, N., Grishchuk, Y., Luthi-Carter, R., Clarke, P.G., Truttmann, A.C., Puyal, J., 2014. Involvement of autophagy in hypoxic-excitotoxic neuronal death. Autophagy 10, 846–860.
Harraz, M.M., Eacker, S.M., Wang, X., Dawson, T.M., Dawson, V.L., 2012. MicroRNA-223 is neuroprotective by targeting glutamate receptors. Proc. Natl. Acad. Sci. U. S. A. 109, 18962–18967.
Hwang, J.-Y., Gertner, M., Pontarelli, F., Court-Vazquez, B., Bennett, M.V.L., Ofengeim, D., Zukin, R.S., 2016. Global ischemia induces lysosomal-mediated degradation of mTOR and activation of autophagy in hippocampal neurons destined to die. Cell Death Differ. 24, 317–329.
Jiang, M., Wang, H., Jin, M., Yang, X., Ji, H., Jiang, Y., Zhang, H., Wu, F., Wu, G., Lai, X., Cai, L., Hu, R., Xu, L., Li, L., 2018. Exosomes from MiR-30d-5p-ADSCs reverse acute ischemic stroke-induced, autophagy-mediated brain injury by promoting M2 microglial/macrophage polarization. Cell. Physiol. Biochem. 47, 864–878.
Jin, K., Mao, X., Xie, L., Galvan, V., Lai, B., Wang, Y., Gorostiza, O., Wang, X., Greenberg, D.A., 2010. Transplantation of human neural precursor cells in Matrigel scaffolding improves outcome from focal cerebral ischemia after delayed postischemic treatment in rats. J. Cerebr. Blood Flow Metabol. 30, 534–544.
Jing, C.h., Wang, L., Liu, P.p., Wu, C., Ruan, D., Chen, G., 2012. Autophagy activation is associated with neuroprotection against apoptosis via a mitochondrial pathway in a rat model of subarachnoid hemorrhage. Neuroscience 213, 144–153.
Johnnidis, J.B., Harris, M.H., Wheeler, R.T., Stehling-Sun, S., Lam, M.H., Kirak, O., Brummelkamp, T.R., Fleming, M.D., Camargo, F.D., 2008. Regulation of progenitor cell proliferation and granulocyte function by microRNA-223. Nature 451, 1125–1129.
Klionsky, D.J., 2010. The autophagy connection. Dev. Cell 19, 11–12.
Le, H.T., Hirko, A.C., Thinschmidt, J.S., Grant, M., Li, Z., Peris, J., King, M.A., Hughes, J.A., Song, S., 2011. The protective effects of plasma gelsolin on stroke outcome in rats. Exp. Transl. Stroke Med. 3, 13.
Li, S.P., He, J.D., Wang, Z., Yu, Y., Fu, S.Y., Zhang, H.M., Zhang, J.J., Shen, Z.Y., 2016. miR-30b inhibits autophagy to alleviate hepatic ischemia-reperfusion injury via decreasing the Atg12-Atg5 conjugate. World J. Gastroenterol. 22, 4501–4514.
Llambi, F., Wang, Y.M., Victor, B., Yang, M., Schneider, D.M., Gingras, S., Parsons, M.J., Zheng, J.H., Brown, S.A., Pelletier, S., Moldoveanu, T., Chen, T., Green, D.R., 2016. BOK is a non-canonical BCL-2 family effector of apoptosis regulated by ER-associated degradation. Cell 165, 421–433.
Longa, E.Z., Weinstein, P.R., Carlson, S., Cummins, R., 1989. Reversible middle cerebral artery occlusion without craniectomy in rats. Stroke 20, 84–91.
Love, S., 2003. Apoptosis and brain ischaemia. Prog. Neuro Psychopharmacol. Biol. Psychiatr. 27, 267–282.
Lv, B., Li, F., Han, J., Fang, J., Xu, L., Sun, C., Hua, T., Zhang, Z., Feng, Z., Jiang, X., 2017. Hif-1α overexpression improves transplanted bone mesenchymal stem cells survival in rat MCAO stroke model. Front. Mol. Neurosci. 10.
Ogawa, A., Mori, E., Minematsu, K., Taki, W., Takahashi, A., Nemoto, S., Miyamoto, S., Sasaki, M., Inoue, T., 2007. Randomized trial of intraarterial infusion of urokinase within 6 hours of middle cerebral artery stroke: the middle cerebral artery embolism local fibrinolytic intervention trial (MELT) Japan. Stroke; a journal of cerebral circulation 38, 2633–2639.
Pan, M., Wang, P., Zheng, C., Zhang, H., Lin, S., Shao, B., Zhuge, Q., Jin, K., 2017. Aging systemic milieu impairs outcome after ischemic stroke in rats. Aging Dis 8, 519–530.
Park, H.K., Chu, K., Jung, K.H., Lee, S.T., Bahn, J.J., Kim, M., Lee, S.K., Roh, J.K., 2009. Autophagy is involved in the ischemic preconditioning. Neurosci. Lett. 451, 16–19.
Pattingre, S., Tassa, A., Qu, X., Garuti, R., Liang, X.H., Mizushima, N., Packer, M., Schneider, M.D., Levine, B., 2005. Bcl-2 antiapoptotic proteins inhibit Beclin 1-dependent autophagy. Cell 122, 927–939.
Ramirez-Lassepas, M., 1998. Stroke and the aging of the brain and the arteries. Geriatrics 53, S44–S48.
Roitbak, T., 2018. Silencing a multifunctional microRNA is beneficial for stroke recovery. Front. Mol. Neurosci. 11, 58.
Ruan, L., Wang, B., ZhuGe, Q., Jin, K., 2015. Coupling of neurogenesis and angiogenesis after ischemic stroke. Brain Res. 1623, 166–173.
Segura, T., Calleja, S., Jordan, J., 2008. Recommendations and treatment strategies for the management of acute ischemic stroke. Expert Opin. Pharmacother. 9, 1071–1085.
Sinoy, S., Fayaz, S.M., Charles, K.D., Suvanish, V.K., Kapfhammer, J.P., Rajanikant, G.K., 2017. Amikacin inhibits mir-497 maturation and exerts post-ischemic neuroprotection. Mol. Neurobiol. 54, 3683–3694.
Strong, K., Mathers, C., Bonita, R., 2007. Preventing stroke: saving lives around the world. Lancet Neurol. 6, 182–187.
Su, J., Zhang, T., Wang, K., Zhu, T., Li, X., 2014. Autophagy activation contributes to the neuroprotection of remote ischemic perconditioning against focal cerebral ischemia in rats. Neurochem. Res. 39, 2068–2077.
Tao, J., Liu, W., Shang, G., Zheng, Y., Huang, J., Lin, R., Chen, L., 2015. MiR-207/352 regulate lysosomal-associated membrane proteins and enzymes following ischemic stroke. Neuroscience 305, 1–14.
Thomenius, M.J., Distelhorst, C.W., 2003. Bcl-2 on the endoplasmic reticulum: protecting the mitochondria from a distance. J. Cell Sci. 116, 4493–4499.
Wang, J., Cao, B., Han, D., Sun, M., Feng, J., 2017. Long non-coding RNA H19 induces cerebral ischemia reperfusion injury via activation of autophagy. Aging Dis 8, 71–84.
Wang, P., Guan, Y.-F., Du, H., Zhai, Q.-W., Su, D.-F., Miao, C.-Y., 2014. Induction of

autophagy contributes to the neuroprotection of nicotinamide phosphoribosyltransferase in cerebral ischemia. Autophagy 8, 77–87.
Wang, P., Shao, B.Z., Deng, Z., Chen, S., Yue, Z., Miao, C.Y., 2018. Autophagy in ischemic stroke. Prog. Neurobiol.
Wei, M.C., Zong, W.X., Cheng, E.H., Lindsten, T., Panoutsakopoulou, V., Ross, A.J., Roth, K.A., MacGregor, G.R., Thompson, C.B., Korsmeyer, S.J., 2001. Proapoptotic BAX and BAK: a requisite gateway to mitochondrial dysfunction and death. Science 292, 727–730.
Wen, Y.D., Sheng, R., Zhang, L.S., Han, R., Zhang, X., Zhang, X.D., Han, F., Fukunaga, K., Qin, Z.H., 2008. Neuronal injury in rat model of permanent focal cerebral ischemia is associated with activation of autophagic and lysosomal pathways. Autophagy 4, 762–769.
Wu, S., Lin, Y., Xu, D., Chen, J., Shu, M., Zhou, Y., Zhu, W., Su, X., Zhou, Y., Qiu, P., Yan, G., 2012. MiR-135a functions as a selective killer of malignant glioma. Oncogene 31, 3866–3874.
Xin, X.Y., Pan, J., Wang, X.Q., Ma, J.F., Ding, J.Q., Yang, G.Y., Chen, S.D., 2011. 2-methoxyestradiol attenuates autophagy activation after global ischemia. Can. J. Neurol. Sci. 38, 631–638.
Xu, L.J., Ouyang, Y.B., Xiong, X., Stary, C.M., Giffard, R.G., 2015. Post-stroke treatment with miR-181 antagomir reduces injury and improves long-term behavioral recovery in mice after focal cerebral ischemia. Exp. Neurol. 264, 1–7.
Xu, X., Wang, B., Ren, C., Hu, J., Greenberg, D.A., Chen, T., Xie, L., Jin, K., 2017. Recent progress in vascular aging: mechanisms and its role in age-related diseases. Aging Dis 8, 486–505.
Yamamoto, A., Yue, Z., 2014. Autophagy and its normal and pathogenic states in the brain. Annu. Rev. Neurosci. 37, 55–78.
Yang, W., Paschen, W., 2017. Is age a key factor contributing to the disparity between success of neuroprotective strategies in young animals and limited success in elderly stroke patients? Focus on protein homeostasis. J. Cerebr. Blood Flow Metabol. 37, 3318–3324.
Yang, Z.B., Zhang, Z., Li, T.B., Lou, Z., Li, S.Y., Yang, H., Yang, J., Luo, X.J., Peng, J., 2014. Up-regulation of brain-enriched miR-107 promotes excitatory neurotoxicity through down-regulation of glutamate transporter-1 expression following ischaemic stroke. Clin. Sci. (Lond.) 127, 679–689.
Yin, K.-J., Deng, Z., Huang, H., Hamblin, M., Xie, C., Zhang, J., Chen, Y.E., 2010. miR-497 regulates neuronal death in mouse brain after transient focal cerebral ischemia. Neurobiol. Dis. 38, 17–26.
Yuan, J., 2009. Neuroprotective strategies targeting apoptotic and necrotic cell death for stroke. Apoptosis 14, 469–477.
Zhang, Z.G., Chopp, M., 2009. Neurorestorative therapies for stroke: underlying mechanisms and translation to the clinic. Lancet Neurol. 8, 491–500.